

I. Stetskiv, V. Kordan, I. Tarasiuk, V. Pavlyuk

Synthesis, Crystal Structure and Physical Properties of the $\text{TbCo}_{4.5}\text{Si}_x\text{Li}_{0.5-x}$ Solid Solution

Ivan Franko National University of Lviv, Lviv, Ukraine, ira.stetskiv95@gmail.com

Alloys from the region of existence of the solid solution $\text{TbCo}_{4.5}\text{Si}_x\text{Li}_{0.5-x}$ were synthesized by arc melting. Quantitative and qualitative composition of alloys and powders of electrode materials was determined by scanning electron microscopy and energy-dispersive X-ray spectroscopy. The Tb/Co/Si ratio in the samples was confirmed by X-ray fluorescence spectroscopy. The change in cell parameters within the solid solution existence was established by the results of X-ray powder diffraction ($\text{TbCo}_{4.5}\text{Si}_x\text{Li}_{0.5-x}$, $x = 0.1 - 0.4$: $a = 4.9518(5) - 4.9324(3)$, $c = 3.9727(4) - 3.9746(3)$ Å). The crystal structure of the solid solution was determined by the Rietveld method (CaCu_5 structure type, space group $P6/mmm$). Cobalt atoms are partially replaced by silicon and lithium only in $2c$ position. The ability of alloys to reversibly absorb hydrogen was studied by the method of electrochemical hydrogenation. Under experimental conditions the amount of deintercalated hydrogen was about 0.19 H/f.u. The change in cell parameters after hydrogenation (volume increases from 83.74(1) to 85.54(6) Å³) and the stability of the electrode in the electrolyte solution was further confirmed by X-ray phase analysis. Measurements of the electrical resistivity of the samples indicated a decrease of resistivity value with a slight increase in the amount of alkali metal in samples.

Keywords: X-ray diffraction; electron microscopy; solid solutions; CaCu_5 -type structure; electrochemical hydrogenation.

Received 28 May 2021; Accepted 6 September 2021.

Introduction

The implementation of renewable energy sources is one of the most important tasks of modern science and industry. Hydrogen energy is one of the most promising options, it is based on the use of hydrogen as energy store. However, creating safe and efficient systems for its storage and transportation is a difficult task, as the use of compressed gaseous or molecular hydrogen carries a lot of risks. The accumulation of hydrogen in the form of hydrides of metals and intermetallic compounds is a possible solution to the above problems. The study of such chemical sources of electric current began after the revealing of the ability of materials such as LaNi_5 , SmCo_5 , FeTi , ZrNi_2 , Mg-based alloys [1] to absorb and desorb hydrogen. After discovering the ability of the LaNi_5 compound to reversibly accumulate hydrogen (up to 6 - 7 H atoms per formula unit) an active study of the properties of compounds belonging to the CaCu_5

structure type and its derivatives has begun [2, 3]. Electrochemical properties of the related to the CaCu_5 -type compounds with framework of Laves phases depend on the type and amount of the doping components. Use of Al, Mg, Mn, Ni, and Co as alloying components results into the improvement of corrosion stability, increasing of life-time and capacity of electrode materials [4 - 8]. Improvement of the hydrogen sorption ability, specific capacity and corrosion potential was observed after the doping of metallic Mg-based electrode with Li and Al [9, 10].

In the case of the hydrogenation of the composite material based on the LaNi_5 and $\text{La}_2\text{Mg}_{17}$ at the first time LaNi_5 sorbs the hydrogen and then plays role of the heterogeneous activator [11]. The characteristics of the hydrogen storage media could be significantly improved by replacing the d -metal atoms with other elements, such as Mn and Al [12, 13]. Al, Ge and Li doping improves thermal stability, corrosion resistance and absorption

capacity during electrochemical hydrogenation of LaCo_5 and LaNi_5 compounds [14]. Addition of a small amount of Li allowed to increase the sorption capacity, while the alloys did not differ in behavior in 6M KOH solution. Partial substitution of Ni for small amounts of Mg and Sb in the LaNi_5 compound causes slight changes in the amount of sorption capacity, while Bi doping increases the amount of absorbed hydrogen up to 6.8 atoms per formula unit [15]. The addition of Sn has the best effect on the absorption of deuterium with a small amount of doping element, while its excess worsens the hydrogenation results for LaNi_5 [16]. The $\text{LaNi}_{4.5}\text{Si}_{0.5}$ alloy shows fast activation and incredibly high stability upon electrochemical cycling (capacity lost is 0.07 mA·h/g for each next cycle); also the electrode is characterized by fairly high electrochemical capacity (245 mA·h/g) [17]. The authors [18] have compared the $\text{LaNi}_{4.7}\text{Al}_{0.3}$, $\text{LaNi}_{4.7}\text{Si}_{0.3}$ and $\text{LaNi}_{4.5}\text{Si}_{0.5}$ phases with the primary LaNi_5 compound and concluded that the improvement of the resource is caused by the mechanical properties of doped materials and increased resistance to disproportionation.

The issues of improving the sorption properties and reducing the cost of chemical sources of electric current continue to be explored by partial or complete substitution of nickel by cobalt or other *d*-elements and lanthanum by other rare earth metals with subsequent *p*- and *s*-elements doping. The aim of our work was to synthesize alloys in the possible region of existence of a $\text{TbCo}_{4.5}\text{Si}_x\text{Li}_{0.5-x}$ substitutional solid solution and to determine the effect of silicon and lithium doping on crystal-chemical and physical properties of the TbCo_5 binary intermetallic compound.

I. Materials and experimental methods

Terbium (Tb), cobalt (Co), silicon (Si) with nominal purities of more than 99.9 wt.% and lithium (Li) with nominal purity of more than 99.8 wt.% were used as the starting materials. Samples weighing 1 g of each were synthesized by arc melting of mixture of pure elements pressed in pellets on a water-cooled copper hearth in purified with a molten titanium getter argon atmosphere, using a tungsten electrode. Since the alloys include a chemically active element (Li), it was added in excess depending on the content of this element in the alloy, but not more than 5%. The control of the alloys compositions was performed by comparing the mass of pellets with the mass of the alloy, the loss during melting did not exceed 5 wt. %. Homogenizing annealing was performed at a temperature of 400 °C for 1 month. The alloys were sealed in evacuated quartz ampoule and annealed in a resistance furnace MP-60 with automatic temperature control with an accuracy of ± 1 °C. Annealed alloys were quenched in cold water without breaking the ampoule.

The main research method was X-ray analysis, which makes it possible to detect the existence of certain phases, determine their cells parameters (X-ray phase analysis), as well as to establish the crystal structure (X-ray structure analysis). Diffraction data were obtained on DRON-2.0M powder diffractometer (FeK_α – radiation).

To determine the quantitative and qualitative composition of alloys and powders of electrode materials the methods of scanning electron microscopy (SEM) and energy-dispersive X-ray spectroscopy (EDX) using a Tescan Vega 3 LMU scanning electron microscope (Oxford Instruments AZtec ONE System) and a REMMA-102-02 scanning electron microscope with an elemental microanalyzer were applied. Determination of the elemental composition (Tb/Co/Si ratio) of the samples by X-ray fluorescence spectroscopy (XRF) was performed on an ElvaX Pro X-ray fluorescence analyzer. X-ray fluorescence spectra were obtained in a pure helium atmosphere because the samples contained a light element (Si).

The efficiency of the electrochemical hydrogenation was investigated in a two-electrode Swagelok-type cell. A synthesized alloy weighing about 0.3 g was used as anode material. It was mixed in powder form with the electrolyte until smooth, then this mixture filled the anode part of the chemical source of electric current prototype. An electrolyte-soaked mixture of freshly prepared nickel(II) hydroxide and graphite (90 and 10% by weight, respectively) was used as the cathode. Graphite was added to improve the conductivity and to reduce dendritic formation. 6M KOH solution was used as the electrolyte. In tested Swagelok-type cell, the cathode and anode were separated by a compressed cellulose separator soaked in the electrolyte solution. Electrochemical measurements were carried out in the galvanostatic mode using MTech G410-2 galvanostat. The charge and discharge processes were performed at a current of 1.0 mA, the total number of charge-discharge cycles was 50.

To investigate the electrical resistivity at low temperatures, the samples were cut on a Struers Accutom-100 cut-off machine. The experiment was performed using the AC measuring technique. Samples with parallel surfaces were attached to a universal holder with four gold wires, cooled with helium down to 4 K and gradually warmed to room temperature.

II. Results and discussion

To investigate the solubility of elements that improve hydrogenation process (Li and Si) in the TbCo_5 binary intermetallic compound, we prepared a series of samples in quaternary system Tb–Co–Si–Li. Before further studies the chemical composition of the synthesized alloys was specified by X-ray fluorescence analysis (Fig. 1). The $\text{TbCo}_{4.5}\text{Si}_{0.2}\text{Li}_{0.3}$ and $\text{TbCo}_{4.5}\text{Si}_{0.1}\text{Li}_{0.4}$ samples were examined by the EDX method. In addition to the main phase with CaCu_5 structure (defined compositions were $\text{Tb}_{15.9(6)}\text{Co}_{79.6(5)}\text{Si}_{4.5(7)}$ and $\text{Tb}_{15.8(5)}\text{Co}_{81.3(6)}\text{Si}_{2.9(6)}$, respectively) both samples contained small amounts of phase with a Gd_2Co_7 structure type ($\text{Tb}_{21.3(5)}\text{Co}_{75.6(3)}\text{Si}_{3.1(6)}$ and $\text{Tb}_{21.3(6)}\text{Co}_{76.6(7)}\text{Si}_{2.1(7)}$, respectively). The overall compositions of alloys and element mapping (Fig. 2) showed that the real composition correlates well with the nominal composition, as well as with the results of the XRF (Li cannot be determined by X-ray spectral methods, so the Tb/Co/Si ratio was taken as a basis).

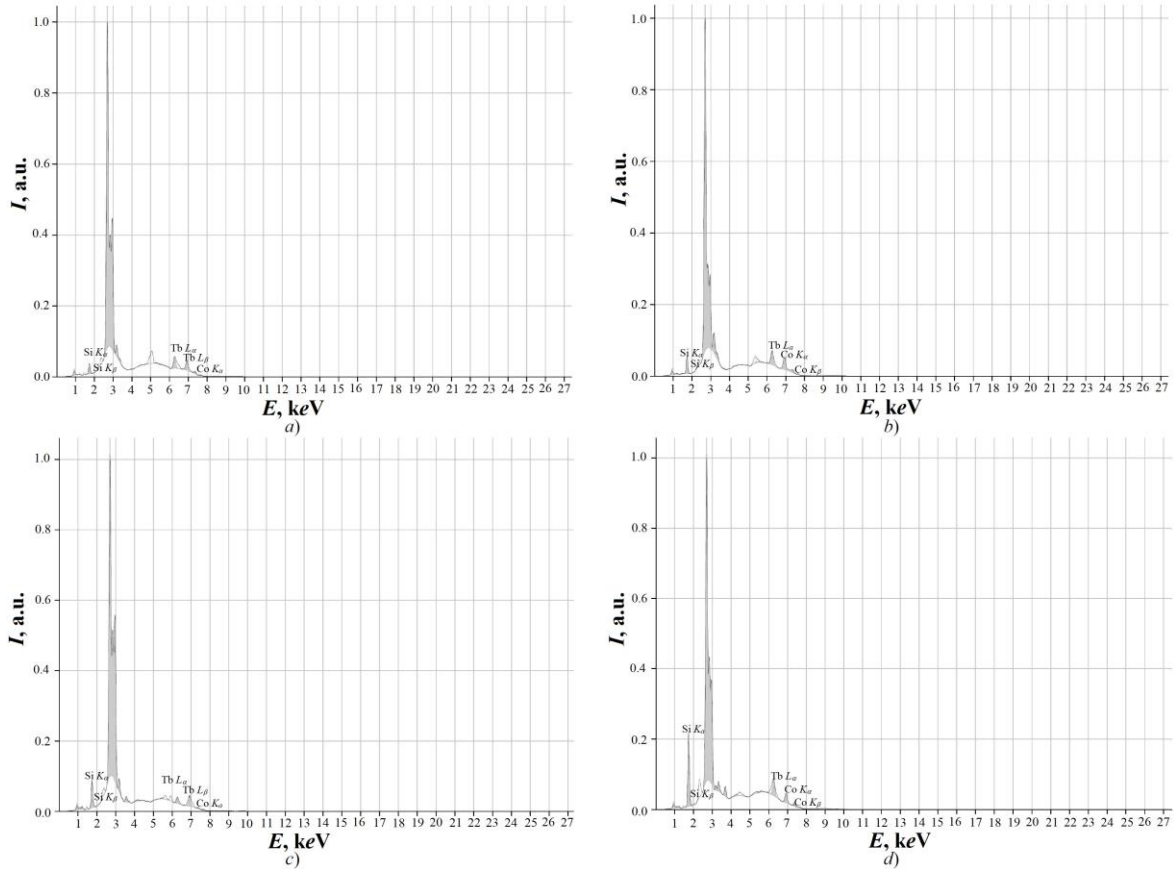


Fig. 1. X-ray fluorescence spectra of the samples: (a) initial composition – $\text{Tb}_{16.67}\text{Co}_{75}\text{Si}_{1.67}\text{Li}_{6.67}$, XRF results – $\text{Tb}_{17.5}\text{Co}_{80.3}\text{Si}_{2.2}$; (b) initial composition – $\text{Tb}_{16.67}\text{Co}_{75}\text{Si}_{3.33}\text{Li}_5$, XRF results – $\text{Tb}_{17.5}\text{Co}_{78.1}\text{Si}_{4.4}$; (c) initial composition – $\text{Tb}_{16.67}\text{Co}_{75}\text{Si}_5\text{Li}_{3.33}$, XRF results – $\text{Tb}_{16.9}\text{Co}_{78.0}\text{Si}_{5.1}$; (d) initial composition – $\text{Tb}_{16.67}\text{Co}_{75}\text{Si}_{6.67}\text{Li}_{1.67}$, XRF results – $\text{Tb}_{16.8}\text{Co}_{75.8}\text{Si}_{7.4}$.

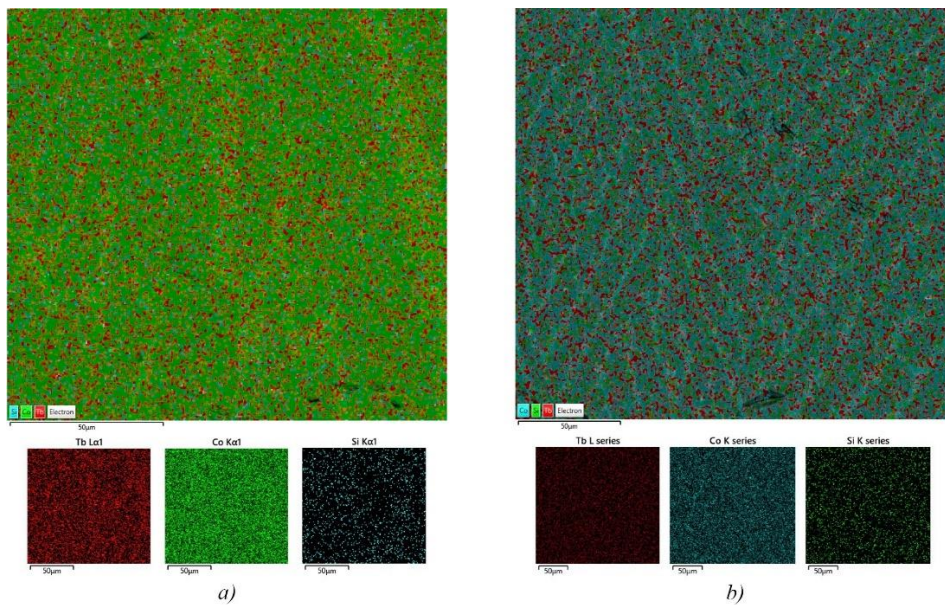


Fig. 2. Elemental distribution maps on the surface of (a) $\text{TbCo}_{4.5}\text{Si}_{0.1}\text{Li}_{0.4}$ (integral composition – $\text{Tb}_{17.3}\text{Co}_{80.5}\text{Si}_{2.2}$) and (b) $\text{TbCo}_{4.5}\text{Si}_{0.2}\text{Li}_{0.3}$ (integral composition – $\text{Tb}_{17.2}\text{Co}_{78.8}\text{Si}_{4.0}$) alloys.

Diffraction patterns of all alloys were obtained and studied by X-ray powder diffraction method. The experimental diffraction patterns of alloys, in which Co was replaced by Si and Li, were compared with the theoretical TbCo_5 diffraction pattern, calculated in the program Powder Cell [20]. As the main phase the samples contain $\text{TbCo}_{4.5}\text{Si}_x\text{Li}_{0.5-x}$ substitutional solid

solution which belongs to the CaCu_5 structure type (space group $P6/mmm$, Pearson symbol $hP6$). The gradual shift of the peaks on the diffraction patterns allowed us to assume the formation of a solid solution.

The crystal structure of the solid solution was refined by the Rietveld method using the JANA2006 program [21]. The atom coordinates of the TbCo_5 compound were

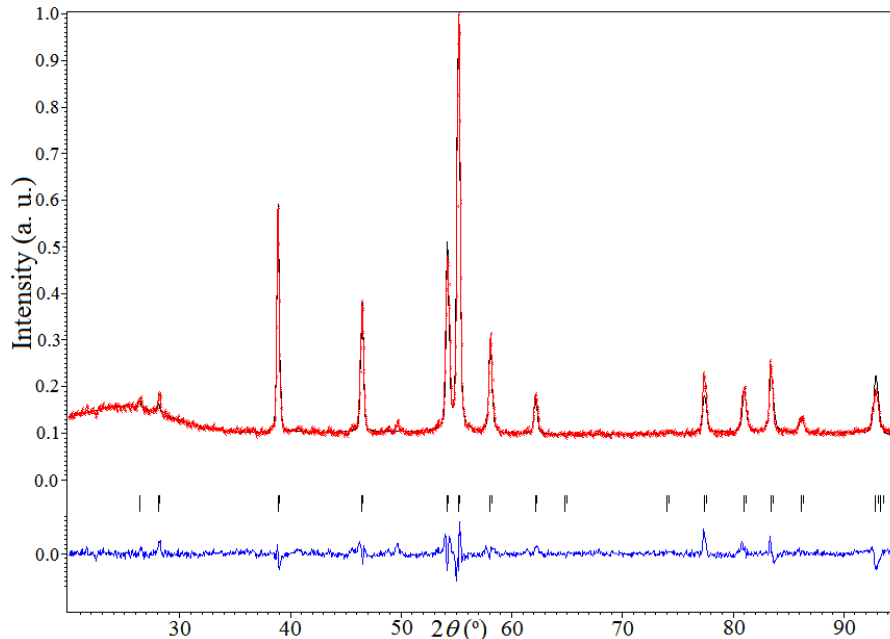


Fig. 3. Calculated (black line), experimental (red) and their difference (blue) diffraction patterns of the $\text{TbCo}_{4.5}\text{Si}_{0.3}\text{Li}_{0.2}$ sample.

Table 1

Atomic coordinates and isotropic displacement parameters of $\text{TbCo}_{4.5}\text{Si}_{0.3}\text{Li}_{0.2}$

Atom	Wyckoff position	x/a	y/b	z/c	$U_i, \text{Å}^2$
Tb	1a	0	0	0	0.055(3)
M^*	2c	1/3	2/3	0	0.022(2)
Co	3g	1/2	0	1/2	0.029(2)

$$M^* = 0.75\text{Co} + 0.15\text{Si} + 0.10\text{Li}$$

used as a model for refinement. Theoretical, experimental and difference between the experimental and theoretical profiles of the diffractogram of the $\text{TbCo}_{4.5}\text{Si}_{0.3}\text{Li}_{0.2}$ sample are shown in Fig. 3. The atom coordinates were refined to the values of the R-factors $R_F = 0.0478$, $R_p = 0.0391$ and $R_{wp} = 0.0523$ and are presented in Table 1.

According to the atomic size, the coordination polyhedron of the largest atom (Tb) is the pseudo-Frank-Kasper polyhedron with coordination number (CN) = 20. The coordination polyhedron of Co atoms is cuboctahedron with CN = 12, and the coordination polyhedron of atoms of statistical mixture is icosahedron with CN = 12. The structure of $\text{TbCo}_{4.5}\text{Si}_x\text{Li}_{0.5-x}$ ($x = 0.1 - 0.4$) and coordination polyhedra of atoms are shown in Fig. 4.

Solid solution is formed by the partial substitution of cobalt atoms by silicon and lithium in 2c position. The cell parameters of different compositions of $\text{TbCo}_{4.5}\text{Si}_x\text{Li}_{0.5-x}$ solid solution ($x = 0.1 - 0.4$) were refined using LATCON [22] and FullProf [23] programs and are given in Table 2. Fig. 5 shows the change of the cell volume within the limits of the solid solution. There is a decrease in a cell parameter with a simultaneous increase in c parameter for the alloy with $\text{TbCo}_{4.5}\text{Si}_{0.3}\text{Li}_{0.2}$ composition. The volume decreases with increasing of silicon content.

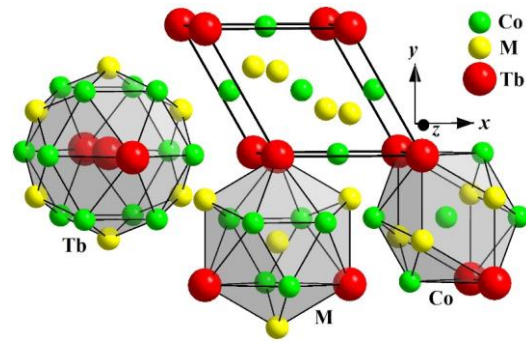


Fig. 4. Unit cell and coordination polyhedra of atoms in the structure of $\text{TbCo}_{4.5}\text{Si}_x\text{Li}_{0.5-x}$ solid solution.

Table 2

Unit cell parameters of the $\text{TbCo}_{4.5}\text{Si}_x\text{Li}_{0.5-x}$ solid solution

Composition	Cell parameters		
	$a, \text{Å}$	$c, \text{Å}$	$V, \text{Å}^3$
$\text{TbCo}_{4.5}\text{Si}_{0.1}\text{Li}_{0.4}$	4.9518(5)	3.9727(4)	84.36(1)
$\text{TbCo}_{4.5}\text{Si}_{0.2}\text{Li}_{0.3}$	4.9496(4)	3.9679(4)	84.18(1)
$\text{TbCo}_{4.5}\text{Si}_{0.3}\text{Li}_{0.2}$	4.9298(7)	3.9804(6)	83.78(2)
$\text{TbCo}_{4.5}\text{Si}_{0.4}\text{Li}_{0.1}$	4.9324(3)	3.9746(3)	83.74(1)

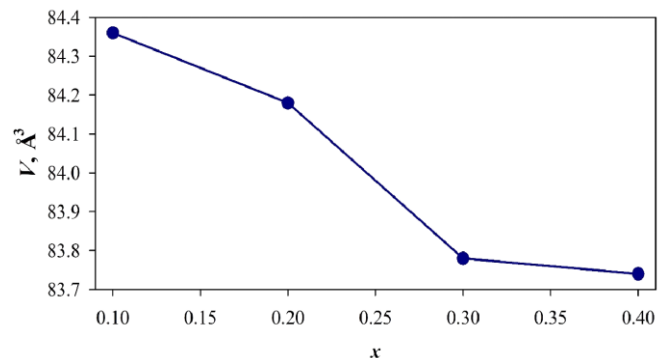


Fig. 5. Unit cell volume change within the $\text{TbCo}_{4.5}\text{Si}_x\text{Li}_{0.5-x}$ ($x = 0.1 - 0.4$) solid solution.

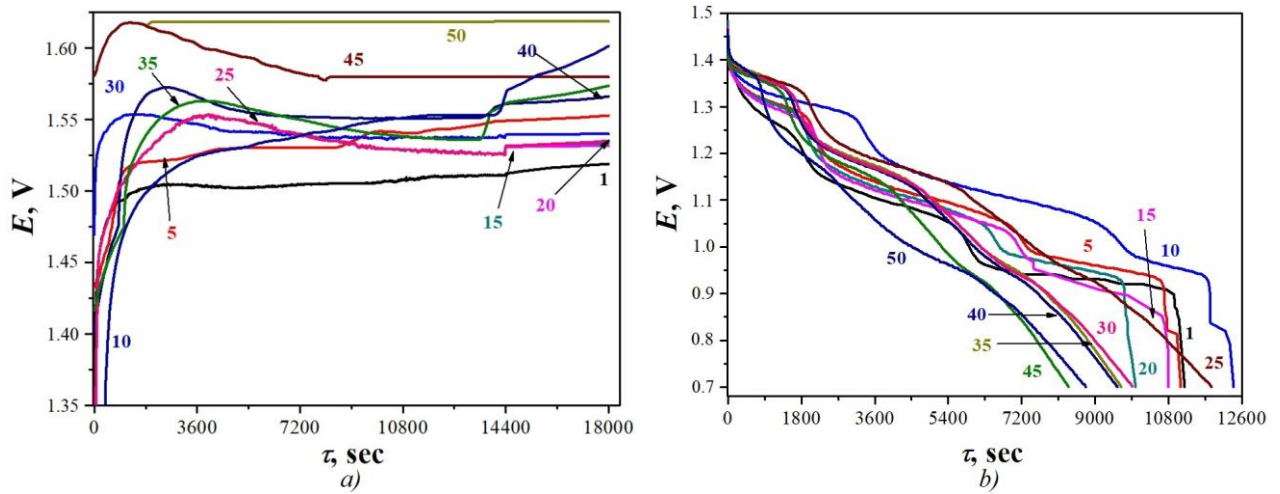


Fig. 6. Selected charge (a) and discharge (b) curves for the Ni-MH battery prototype with the $\text{TbCo}_{4.5}\text{Si}_{0.4}\text{Li}_{0.1}$ -based electrode.

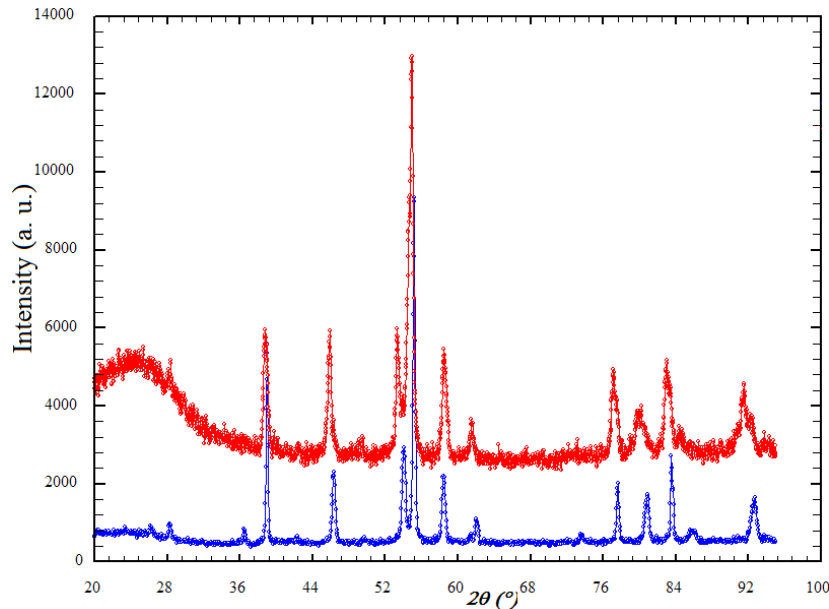


Fig. 7. X-ray powder patterns of the $\text{TbCo}_{4.5}\text{Si}_{0.4}\text{Li}_{0.1}$ (bottom) and $\text{TbCo}_{4.5}\text{Si}_{0.4}\text{Li}_{0.1}\text{H}_x$ (top) samples.

We performed electrochemical hydrogenation of the $\text{TbCo}_{4.5}\text{Si}_{0.4}\text{Li}_{0.1}$ alloy from the region of solid solution existence. The charge curves are shown in Fig. 6a, discharge – in Fig. 6b. The ordinal number of the charge-discharge cycle is marked.

There are several plateaus on the charge-discharge curves, which indicates a specific interaction of the alloy surface with the electrolyte and the formation of passivating amorphous films. The dehydrogenation process occurs at the values of the discharge plateau potential 1.40 - 0.95 V. Other plateaus (at lower potentials) correspond to secondary reversible processes of electrode passivation. The cell parameters changed from $a = 4.9324(3)$, $c = 3.9746(3)$ Å (before hydrogenation) to $a = 4.986(2)$, $c = 3.973(2)$ Å (after hydrogenation), cell volume increased from 83.74(1) to 85.54(6) Å³. An electrode based on a two-component $\text{Tb}_{16.7}\text{Co}_{83.3}$ alloy demonstrates similar electrochemical behaviour, but we observe a much higher nominal

discharge voltage after doping by Li and Si, as in the case of indium and zinc alloying components [24, 25]. Slightly broad peaks observed on the diffraction pattern after electrochemical hydrogenation (Fig. 7) suggest partial amorphization of the anode material. The amount of deintercalated hydrogen under experimental conditions was about 0.19 H/f.u. It must be recognized, that partial cobalt substitution by germanium and lithium leads to worse results [26].

According to the results of energy dispersive X-ray spectroscopy (Fig. 8a) the $\text{TbCo}_{4.5}\text{Si}_{0.4}\text{Li}_{0.1}$ alloy is single-phase and its obtained composition is $\text{Tb}_{16.8}\text{Co}_{77.3}\text{Si}_{5.9}$. The formation of a porous surface on the grains of the investigated alloy was observed after electrochemical hydrogenation (Fig. 8b), chemical composition of the anode material following EDX data is $\text{Tb}_{15.2}\text{Co}_{78.0}\text{Si}_{6.8}$.

The $\text{TbCo}_{4.5}\text{Si}_{0.2}\text{Li}_{0.3}$ and $\text{TbCo}_{4.5}\text{Si}_{0.1}\text{Li}_{0.4}$ samples were selected to study the electrical resistivity. The

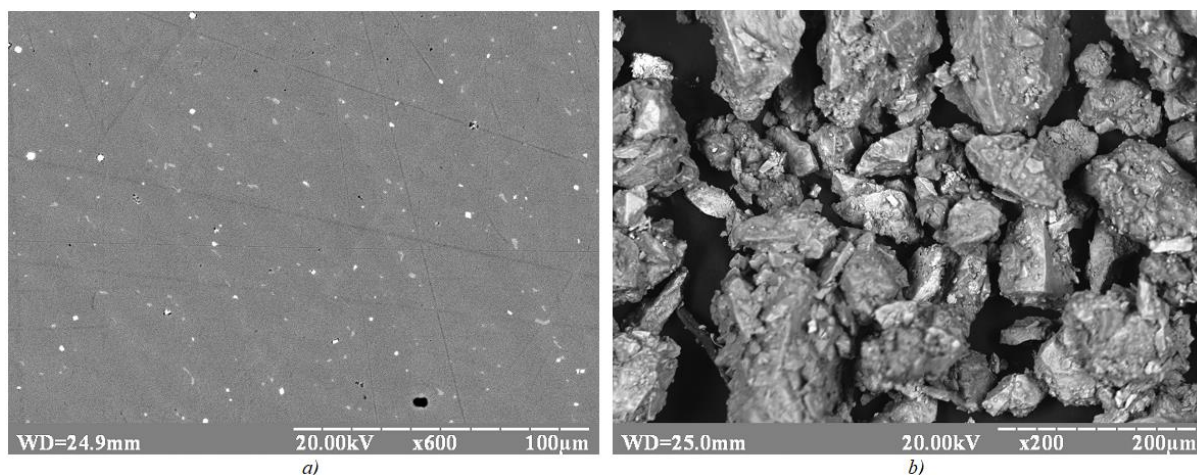


Fig. 8. Microstructure of the $\text{TbCo}_{4.5}\text{Si}_{0.4}\text{Li}_{0.1}$ alloy (a) and SEM-image of the electrode material (b) after the hydrogenation process (gray phase – $\text{Tb}_{15.2}\text{Co}_{78.0}\text{Si}_{6.8}$).

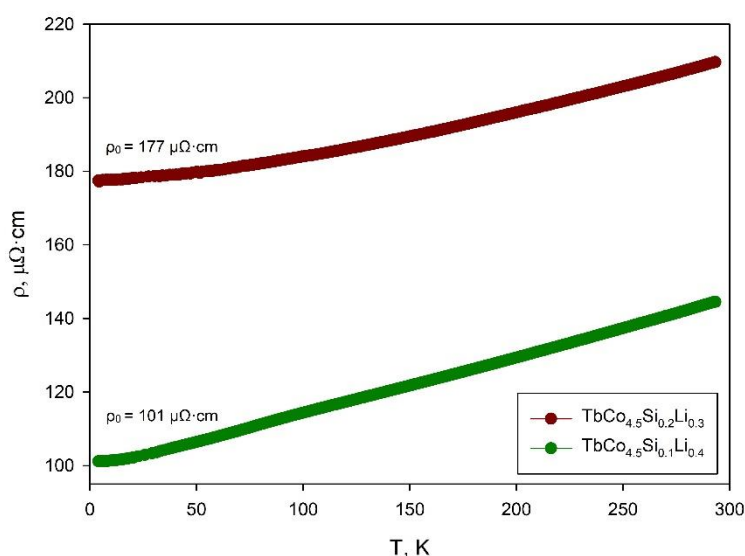


Fig. 9. Electrical resistivity of the $\text{TbCo}_{4.5}\text{Si}_{0.1}\text{Li}_{0.4}$ (bottom) and $\text{TbCo}_{4.5}\text{Si}_{0.2}\text{Li}_{0.3}$ (top) samples.

results of conducting measurements are presented in Fig. 9. A close to the rectilinear dependence of the increase in electrical resistivity with increasing temperature is observed, as expected. While a slight increase in the amount of alkali metal in the alloy leads to a decrease in the values of resistivity.

Conclusions

The existence of a solid solution of $\text{TbCo}_{4.5}\text{Si}_x\text{Li}_{0.5-x}$ with cell parameters from $a = 4.9518(5)$, $c = 3.9727(4)$ Å ($x = 0.1$) to $a = 4.9324(3)$, $c = 3.9746(3)$ Å ($x = 0.4$) was revealed using energy-dispersive X-ray spectroscopy, X-ray fluorescence and X-ray powder diffraction methods. With increasing of silicon content in the sample

the volume decreases nonlinearly. It was established that the substitution of Co atoms by Si and Li atoms occurs only in Wyckoff position 2c. The hydride for the sample with composition $\text{TbCo}_{4.5}\text{Si}_{0.4}\text{Li}_{0.1}$ was synthesized electrochemically and it was determined that under experimental conditions the amount of deintercalated hydrogen was about 0.19 H/f.u. According to the results of the electrical resistivity measurements, it was found that it decreases with a slight increase in the amount of alkali metal in the alloys.

Stetskiv I.A. – PhD student;
Kordan V.M. – PhD, Research Fellow;
Tarasiuk I.I. – PhD, Research Fellow;
Pavlyuk V.V. – DSc, Professor.

- [1] M.H. Mintz, I. Javob, D. Shaltiel, L. Schlapbach (Eds.), Hydrogen in Intermetallic Compounds II (Springer, Berlin, 1992).
- [2] H.H. Van Mal, K.H.J. Buschow, A.R. Miedema, J. Less. Common. Met. 35(1), 65 (1974); [https://doi.org/10.1016/0022-5088\(74\)90146-5](https://doi.org/10.1016/0022-5088(74)90146-5).

- [3] H.H. Van Mal, K.H.J. Buschow, F.A. Kuijpers, J. Less. Common. Met. 32(2), 289 (1973); [https://doi.org/10.1016/0022-5088\(73\)90095-7](https://doi.org/10.1016/0022-5088(73)90095-7).
- [4] Yu. Liu, H. Yuan, M. Guo, M. Jiang, Int. J. Hydrog. Energy 44, 22064 (2019); <https://doi.org/10.1016/j.ijhydene.2019.06.081>.
- [5] L. Wang, X. Zhang, Sh. Zhou, J. Xu, H. Yan, Qu. Luo, Qi. Li, Int. J. Hydrog. Energy 45, 16677 (2020); <https://doi.org/10.1016/j.ijhydene.2020.04.136>.
- [6] N.O. Chorna, V.M. Kordan, A.M. Mykhailevych, O.Ya. Zelinska, A.V. Zelinskiy, K. Kluziak, R.Ya. Serkiz, V.V. Pavlyuk, Voprosy khimii i khimicheskoi tekhnologii, 2, 139 (2021); <https://doi.org/10.32434/0321-4095-2021-135-2-139-149>.
- [7] J. Liu, Sh. Zhu, H. Cheng, Zh. Zheng, Zh. Zhu, K. Yan, Sh. Han, J. Alloys Compd. 777, 1087 (2019); <https://doi.org/10.1016/j.jallcom.2018.11.094>.
- [8] A. Stetskiv, I. Tarasiuk, R. Misztal, V. Pavlyuk, Acta Crystallogr. E 67, 61 (2011); <https://doi.org/10.1107/S1600536811041328>.
- [9] V. Pavlyuk, W. Ciesielski, N. Pavlyuk, D. Kulawik, M. Szyrej, B. Rozdzynska-Kielbik, V. Kordan, Ionics 25(6), 2701 (2019); <https://doi.org/10.1007/s11581-018-2743-8>.
- [10] V. Pavlyuk, W. Ciesielski, N. Pavlyuk, D. Kulawik, G. Kowalczyk, A. Balińska, M. Szyrej, B. Rozdzynska-Kielbik, A. Folentarska, V. Kordan, Mater. Chem. Phys. 223, 503 (2019); <https://doi.org/10.1016/j.matchemphys.2018.11.007>.
- [11] K. Dutta, O. N. Srivastava, J. Mater. Sci. 28, 3457 (1993); <https://doi.org/10.1007/BF01159822>.
- [12] A. Percheron-Guégan, C. Lartigue, J. C. Achard, P. Germi, F. Tasset, J. Less. Common. Met. 74(1), 1 (1980); [https://doi.org/10.1016/0022-5088\(80\)90063-6](https://doi.org/10.1016/0022-5088(80)90063-6).
- [13] W. Zhou, Zh. Ma, Ch. Wu, D. Zhu, L. Huang, Yu. Chen, Int. J. Hydrog. Energy 41, 1801 (2016); <https://doi.org/10.1016/j.ijhydene.2015.10.070>.
- [14] A. Stetskiv, B. Rożdżyńska-Kielbik, G. Kowalczyk, W. Prochwicz, P. Siemion, V. Pavlyuk, Solid State Sci. 38, 35 (2014); <https://doi.org/10.1016/j.solidstatesciences.2014.09.016>.
- [15] K. Giza, W. Iwasieczko, V. V. Pavlyuk, H. Bala, H. Drulis, J. Power Sources. 181(1), 38 (2008); <https://doi.org/10.1016/j.jpowsour.2007.12.018>.
- [16] J.-M. Joubert, M. Latroche, R. Černý, R. C. Bowman, A. Percheron-Guégan, K. Yvon, J. Alloys. Compd. 293-295, 124 (1999); [https://doi.org/10.1016/S0925-8388\(99\)00311-4](https://doi.org/10.1016/S0925-8388(99)00311-4).
- [17] F. Meli, A. Zuetzel, L. Schlapbach, Z. Phys. Chem. 183(1-2), 371 (1994); https://doi.org/10.1524/zpch.1994.183.Part_1_2.371.
- [18] F. Meli, A. Zuetzel, L. Schlapbach, J. Alloys. Compd. 190(1), 17 (1992); [https://doi.org/10.1016/0925-8388\(92\)90167-8](https://doi.org/10.1016/0925-8388(92)90167-8).
- [19] MTech. Retrieved from: <http://chem.lnu.edu.ua/mtech/mtech.htm>.
- [20] W. Kraus, G. Nolze, PowderCell for Windows (Federal Institute for Materials Research and Testing, Berlin, 2000).
- [21] V. Petříček, M. Dušek, L. Palatinus, Z. Kristallogr. Cryst. Mater. 229(5), 345 (2014); <https://doi.org/10.1515/zkri-2014-1737>.
- [22] D. Schwarzenbach, Program LATCON: refine lattice parameters. (University of Lausanne, Lausanne, 1966).
- [23] J. Rodriguez-Carvajal, The Satellite Meeting on Powder Diffraction of the XV Congress of the IUCr (Toulouse, 1990). P. 127.
- [24] V. Kordan, I. Tarasiuk, I. Stetskiv, R. Serkiz, V. Pavlyuk, Chem. Met. Alloys. 12(3/4), 77 (2019); <https://doi.org/10.30970/cma12.0396>.
- [25] B. Rożdżyńska-Kielbik, I. Stetskiv, V. Pavlyuk, A. Stetskiv, Solid State Sci. 113, 106552 (2021); <https://doi.org/10.1016/j.solidstatesciences.2021.106552>.
- [26] I. Tarasiuk., I. Stetskiv, V. Kordan., V. Pavlyuk, Visn. Lviv Univ. Ser. Chem. 58(1), 117 (2017).

І. Стецьків, В. Кордан, І. Тарасюк, В. Павлюк

Синтез, кристалічна структура та фізичні властивості твердого розчину $\text{TbCo}_{4,5}\text{Si}_x\text{Li}_{0,5-x}$

Львівський національний університет імені Івана Франка, Львів, Україна, ira.stetskiv95@gmail.com

Методом електродугового плавлення синтезовано сплави з області існування твердого розчину $\text{TbCo}_{4,5}\text{Si}_x\text{Li}_{0,5-x}$. За допомогою скануючої електронної мікроскопії та енергодисперсійної рентгенівської спектроскопії визначено кількісний і якісний склад сплавів та порошків електродних матеріалів. Співвідношення Tb/Co/Si у зразках підтверджено рентгенофлуоресцентною спектроскопією. Зміну параметрів комірки у межах твердого розчину встановлено за результатами рентгенівської порошкової дифракції ($\text{TbCo}_{4,5}\text{Si}_x\text{Li}_{0,5-x}$, $x = 0,1 - 0,4$: $a = 4,9518(5) - 4,9324(3)$, $c = 3,9727(4) - 3,9746(3)$ Å). Кристалічну структуру твердого розчину визначено методом Рітвельда (структурний тип CaCu_5 , просторова група $R\bar{6}/mmm$). Атоми Кобальту частково заміщуються на Силіцій і Літій тільки у положенні 2c. Методом електрохімічного гідрування досліджено здатність сплавів до поглинання водню, за умов експерименту деінтеркалюється до 0,19 Н/ф.о. Зміну параметрів комірки після гідрування (об'єм зростає від 83,74(1) до 85,54(6) Å³) і стійкість електроду у розчині електроліту додатково підтверджено за результатами рентгенофазового аналізу. Вимірювання питомого електроопору зразків вказали на його зменшення при незначному збільшенні кількості лужного металу.

Ключові слова: рентгенівська дифракція, електронна мікроскопія, тверді розчини, структурний тип CaCu_5 , електрохімічне гідрування.